# Optimization of the Combined Delayed Neutron and Differential Die-Away Prompt Neutron Signal Detection for Characterization of Spent Nuclear Fuel Assemblies – 11419

Pauline Blanc,[1]* Stephen J. Tobin[1], Stephen Croft,[1] Howard O. Menlove,[1] Martyn T. Swinhoe,[1] Taehoon Lee[2]

[1]Los Alamos National Laboratory, Los Alamos, NM 87545, USA
[2]Korea Atomic Energy Research Institute, Yuseong-gu, Daejeon, South Korea, 305-353

## Abstract

The Next Generation Safeguards Initiative (NGSI) of the U.S. Department of Energy (DOE) has funded multiple laboratories and universities to develop a means to accurately quantify the Plutonium (Pu) mass in spent nuclear fuel assemblies and ways to also detect potential diversion of fuel pins. Delayed Neutron (DN) counting provides a signature somewhat more sensitive to $^{235}$U than Pu while Differential Die-Away (DDA) is complementary in that it has greater sensitivity to Pu. The two methods can, with care, be combined into a single instrument which also provides passive neutron information. Individually the techniques cannot robustly quantify the Pu content but coupled together the information content in the signatures enables Pu quantification separate to the total fissile content. The challenge of merging DN and DDA, prompt neutron (PN) signal, capabilities in the same design is the focus of this paper. Other possibilities also suggest themselves, such as a direct measurement of the reactivity (multiplication) by either the boost in signal obtained during the active interrogation itself or by the extension of the die-away profile. In an early study, conceptual designs have been modeled using a neutron detector comprising fission chambers or $^{3}$He proportional counters and a ~14 MeV neutron Deuterium-Tritium (DT) generator as the interrogation source. Modeling was performed using the radiation transport code Monte Carlo N-Particles eXtended (MCNPX). Building on this foundation, the present paper quantifies the capability of a new design using an array of $^{3}$He detectors together with fission chambers to optimize both DN and PN detections and active characterization, respectively. This new design was created in order to minimize fission in $^{238}$U (a nuisance DN emitter), to use a realistic neutron generator, to reduce the cost and to achieve near homogeneous spatial interrogation and detection of the DN and PN, important for detection of diversion, all within the constraints of a single practical instrument. Both DN and PN detections are active techniques using the signal from the most prominent fissile isotopes of spent nuclear fuel that respond the best to a slow neutron interrogation, $^{235}$U, $^{239}$Pu and $^{241}$Pu. The performance is characterized against a library of 64 assemblies and 27 diversion scenarios at different burnup (BU), cooling-time (CT) and initial enrichment (IE) in fresh water.

## Introduction

The Next Generation Safeguards Initiative[1] (NGSI) of the U.S. Department of Energy (DOE) has funded a multi-laboratory/university collaboration to quantify the plutonium (Pu) mass and to detect diversion of pins from spent nuclear fuel assemblies (SFA). This paper quantifies the capability of the Delayed Neutron (DN) active Non-Destructive Assay (NDA) technique using $^{3}$He counters and a ~14 MeV Deuterium-Tritium (DT) neutron generator in an integrated DN and differential die-away (DDA), prompt neutron (PN) signal, system. Recent publications provide details of the motivations[2] and approaches[3] being taken by the NGSI research effort.[4,5,6]

## Concept of Delayed Neutron Assay

DN counting is an active assay technique that consists of turning on and off an interrogating source, in this case the DT generator, and counting DN emitted when the source is off.[7] The details of this technique together with preliminary results are given in a publication by Blanc et al.[8] The time dependence of emitted DN from the many

*Email: pblanc@lanl.gov

precursors produced is described by only six groups[9] in the Monte Carlo code MCNPX[15] which has effective half-lives varying from ~0.2 sec to ~1 minute. The use of 8 groups[13] or other energy structures[14] will not affect overall conclusions significantly. The following interrogation pattern was repeated 150 times: 0.9 s interrogation, 0.1 s pause, 1.0 s count time. The safeguards goal of interest to this work is quantifying the mass of elemental Pu. The DN instrument was designed to emphasize the signal from fissile isotopes relative to fertile isotopes since the fertile signal would be dominated by $^{238}$U in spent fuel which would reduce our ability to quantify Pu. Through integration with other NDA instruments such as DDA, the fissile Pu will be used to determine elemental Pu through, for example, PN/DN ratio. The DN instrument preferentially measures $^{235}$U relative to $^{239}$Pu. This is due to the fact that the microscopic cross section delayed neutron yield ($\beta\nu\sigma_f$) of $^{235}$U is ~2 times larger per fission than $^{239}$Pu at thermal energies.[7] $^{241}$Pu has a delayed-neutron fraction that is very similar to $^{235}$U and a microscopic cross section delayed neutron yield which is ~1.7 times as large as $^{235}$U and so the clarity of discrimination between $^{235}$U and $^{239}$Pu will be reduced.[10] However, given that the mass of $^{241}$Pu is significantly smaller[12] than $^{235}$U in spent fuel, the emphasis remains. Both fissile and fertile isotopes produce delayed neutrons where $^{235}$U, $^{239}$Pu and $^{241}$Pu are the prominent fissile and $^{238}$U is the dominant fertile. Fission in $^{238}$U can be a significant issue since it has the largest mass[12] of any isotope in the fuel. Given that the goal of the NGSI Spent Fuel effort is to quantify the Pu mass and that $^{238}$U comprises ~ 95% of the actinide mass, the design of the instrument has to minimize fission in $^{238}$U by implementing spectrum tailoring and the ratio fissile to fertile has to be increased in order to decrease the uncertainty on the results.

In this study we came to the conclusion that in a water media, the spectrum tailoring materials used don't have as much influence as the water itself since most of the fertile signal comes from induced fissile fission neutrons happening within the fuel assembly rather than from source neutron (SN) inducing fission in $^{238}$U. This leads to the concept of an "active background". Both backgrounds are from signals considered non-proportional to the fissile content.

The "passive background" is mainly from spontaneous fission of $^{244}$Cm amplified by induced fission neutrons owing to the fact that SFAs have multiplication factors of ~ x2 to x4.

The "active background" is: (1) From fissions in $^{238}$U induced by source neutrons after the DT interrogation. This amount should be very small especially when spectrum tailoring is implemented and the media is water ($\sigma_{f_U\text{-}238}$ > 1 MeV[11] and the neutron flux at the entry of the assembly mainly < 1 MeV as shown later). In DDA (PN) delayed time gate, this signal is negligible since PN coming from $^{238}$U fissions induced by SN are gone after ~2 μs while the data acquisition would start after 2 μs as shown later; (2) From fissions in $^{238}$U induced by PN emitted after fissions in $^{238}$U induced by SN from the DT burst. This amount should also be relatively small.

The actual delayed neutron signal comes from: (1) Fast fissions in fissile induced by SN. This represents a small amount in water and when spectrum tailoring implemented but could be a complication when the amount increases since the DN yield is energy dependant; (2) Thermal fissions in the fissile isotopes which is the main signal with multiplication in the assembly; (3) Fissions in fissile induced by the fission-spectrum from fissions in fissile, this amount is much smaller, with multi-generation, (4) Fissions in $^{238}$U from the fission-spectrum from fissions in fissile is a large fraction of the signal and of the mass with multi-generations of neutrons.

Note, in this study the active background from $^{238}$U hasn't been isolated from the actual signal but should be determined, especially when exploring the instrument in other less moderating media. In water, the actual DN signal dominates the "active background", however, in borated water (such as in storage pools at reactor sites) it changes by a factor of ~2. Furthermore, at high burnups (BU), absorbers add uncertainties to calculated ratio. In Figure 1, DN spectra are provided through MCNPX[15] simulations for the 3 main fissile and main fertile. The spectra provided are for incident neutron energies below and above $^{238}$U fission cross section threshold.[11]

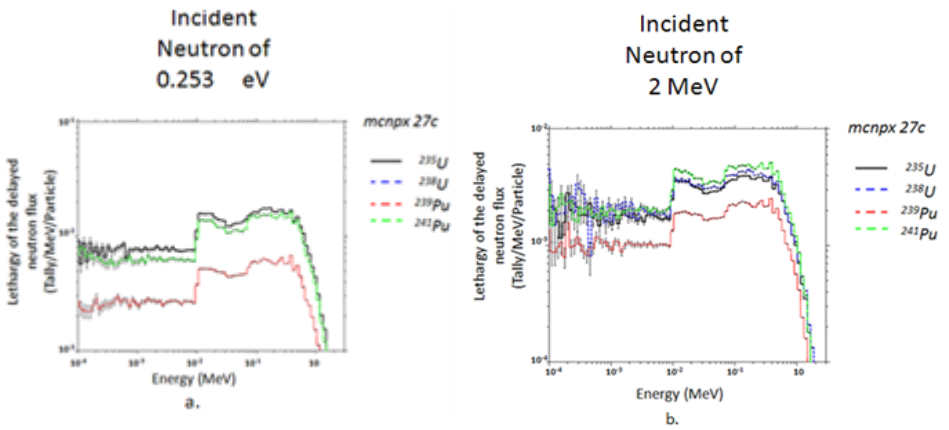


Figure 1: a. and b. represent the DN spectra (tally/MeV/particles) (in MCNPX 27c[15]) as a function of energy (MeV) for the 3 main fissile $^{235}$U, $^{239}$Pu and $^{241}$Pu and main fertile $^{238}$U respectively for an incident neutron energy of 0.253 MeV and 2 MeV.

Figure 1 shows well the importance of spectrum tailoring since by decreasing the neutron energy spectrum $^{238}$U fission from source neutrons could be suppressed.

**Concept of the differential die-away Assay**

The DDA technique is an active assay. The prompt neutron (PN) population of induced fissions following a DT shot dies away with a certain decay time after an interrogation pulse tracking the thermal interrogation flux. The die-away time varies according to the fissile content of the target material and the surrounding media, water, air or borated water. It provides a unique signature to the fissile content of the interrogated SFA. The detected signal in the Cadmium wrapped $^{3}$He detectors surrounding the fuel assembly is insensitive to thermal interrogating neutrons. Thus, the signal of interest comes from fast PN. Further details and preliminary results are provided in a publication by Lee et al.[16] The die-away time and the PN population increase with the amount of fissile hence a larger DDA signal achieved. Among various fissile components, 3 major thermal-induced fission isotopes contribute to the signal, $^{235}$U, $^{239}$Pu and $^{241}$Pu. Neutron absorbers include not only 12 dominant fission fragment poisons such as $^{99}$Tc, $^{131}$Xe, $^{133}$Cs, $^{143}$Nd, $^{145}$Nd, $^{149}$Sm, $^{150}$Sm, $^{151}$Sm, $^{151}$Eu, $^{154}$Eu, $^{155}$Gd, $^{157}$Gd, but also fertile such as $^{238}$U and $^{240}$Pu. The neutron energy spectrum of spectrum-tailored ~14 MeV DT neutrons at the outer surface of spectrum tailoring materials adjacent to the SFA for different time zones was calculated[16] with MCNPX[15] as shown in Figure 2. The spectrum tailoring is achieved through tungsten (W) and beryllium (Be) in the papers by T. Lee et al.[16] and P. Blanc et al.[8] However, these calculations have been compared to the present design (tungsten and stainless steel considered easier to fabricate) and the trends found to be similar.

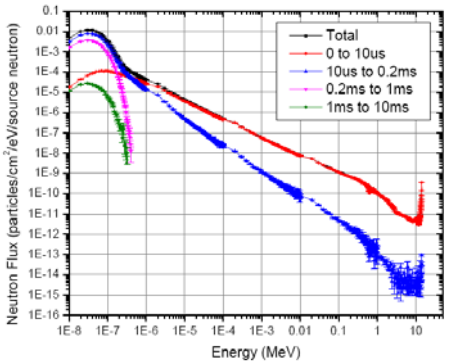


Figure 2: Energy spectrum of ~14 MeV SN thermalized by spectrum tailoring materials, W & Be[16] for different time zones.

We can see that most of ~14 MeV neutrons from the DT generator are reduced to thermal energies during the initial interrogation time (0 to 10 μs), and thus, more than 90% of the source neutrons are shifted below 1 MeV through spectrum tailoring as displayed later. The neutron population decrease, after interrogation, falls off with a specific die-away time varying as a function of the SFA. The neutron die-away time for a pure $^{238}UO_2$ assembly (i.e. no fissile materials) is much shorter than those of the other SFAs. This is due to the sustaining time of chain reactions in $^{238}U$ being much shorter than those of fissile isotopes.

**Time control of DDA and DN data acquisition**

With a proper control of the timing, the DN-DDA instrument could be use for both applications. An example is given in Figure 3, (1) an interrogation pulse is generated from 0 to 10 μs, (2) waiting for DT source neutrons and induced PN from fission in $^{238}U$ to be thermalized, (3) data acquisition for DDA from 0.2 to 1 ms where most of detected neutrons are fast, (4) waiting until PN die away, (5) data acquisition for DN from 5 to 10 ms. This pattern could be repeated for 300 s with a frequency of 100 Hz.

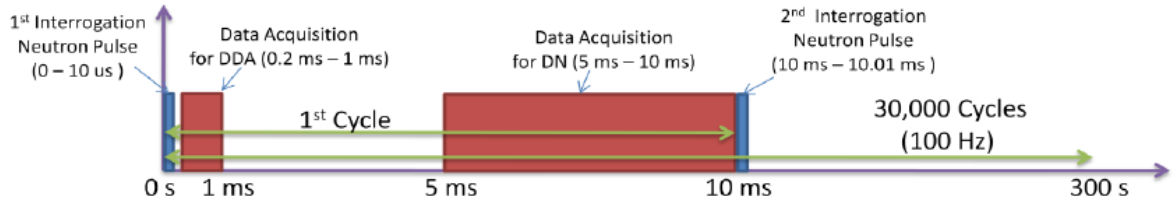


Figure 3: Timing control example for interrogation neutron pulse and data acquisitions for DDA and DN applications.

DDA and DN are performed separately, as if in separate assays, and thus, in the simulation aren't done respecting this time frame, but the conclusions remain applicable to this pattern when actually integrating both instruments.

**Design Requirements in the Context of an Integrated DN-DDA Instrument**

A 17 by 17 Westinghouse PWR assembly was selected to quantify the capability of all techniques in the NGSI[1] Spent Fuel effort. Differences among assemblies emphasized isotopic, spatial, and diversion variability.[17] The isotopic variability among 64 assemblies was obtained by using the Monte Carlo N-Particle eXtended (MCNPX) transport code[15] that recently had the CINDER BU capability added.[12] The spatial variability is only in the horizontal direction, no axial variation was quantified.[12] Each of the 264 pin rods were divided into 4 separate radial cells to allow for radial variation of Pu peaking on the edge of the pellet. This level of resolution within one pin isn't expected to produce a significant effect on a DN instrument which has good penetration and uniformity. BU differences among pins center to edge should be more important. Any realistic instrument will only measure an axial segment and respond essentially to local concentration or linear density but this isn't a hindrance to our assessment. The present design hasn't yet been fully optimized since research is ongoing and different requirements of a potential integration aren't yet finalized. The design in Figure 4 uses a DT generator and 7 $^{3}He$ gas filled proportional counters. The main goal of such a design for DN counting is to decrease the neutron energy spectrum[18] to reduce fission in $^{238}U$. Spectrum tailoring is created through tungsten and stainless steel (SS) around the neutron generator. Stainless Steel will be used as a reflector. The pin array is ~366 cm long and 21.58 by 21.58 cm across. The medium surrounding the pins is water. On all sides of the SFA is a 0.5 cm gap filled with water needed to provide the mechanical tolerance for moving an assembly through the detector. Blocks of Lead surround the SFA and the detectors which are also encased in High Density Polyethylene (HDPE) blocks. To increase the DN signal efficiency, 3 detectors haven't been wrapped in Cd where 4 others have for DDA (PN) applications.

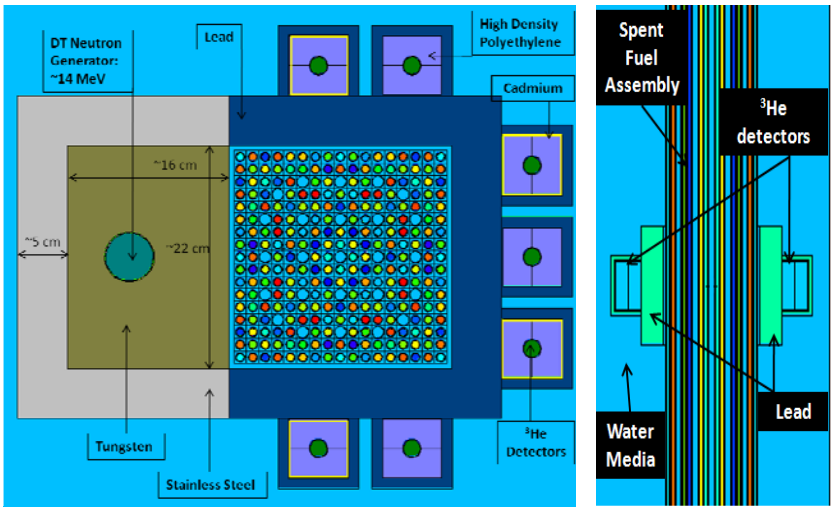


Figure 4: From left to right, XY slice of the design using W and SS for spectrum tailoring, vertical (Z) cross section in water.

All detectors are comprised of $^{3}$He gas in an aluminum cylinder, 5.08 cm long (active length), and 0.945 cm in radius. $^{3}$He tubes are encased in 6 x 6 x 9.28 cm HDPE blocks, 4 of them (Yellow outlines in Figure 4) are surrounded by Cd liners 0.1 cm thick and 9.28 cm tall. The whole is embedded in a 5.89 x 5.89 x 11.28 cm lead block centered in the middle of the assembly in the Z direction. The DT target is located in a 9.8 cm tall cylinder of 2.4 cm radius surrounded by a ~16.25 x 22.4 x 20 cm W block surrounded by a ~21.25 x 32.4 x 27 cm block of SS. In Figure 5 the neutron energy spectrum at the entry of the SFA, before neutrons enter the water surrounding the array of 17x17 fuel pins is shown, fluxes are strictly for reaching the external surface of Be from T. Lee et al.[16] and W & SS (respectively D1 and D2 in Figure 4). The results below are the directional flux entering the SFA by making all cells outside of the generator (DT, W, SS) void in the simulation and killing all returning neutrons.

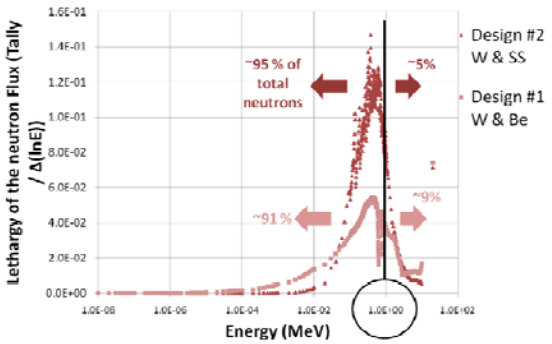


Figure 5: Red and pink plots represent the lethargy of the neutron fluxes per SN at the entry of the surfaces of respectively D1[16] (Be) and D2 (W & SS) before entering the water. The results are obtained in MCNPX[15] (v27c). Incoming flux only.

Both spectrum tailoring designs (W & Be) and D2 (W & SS) have similar impact on the proportion and intensity of SN entering the fuel with an energy below 1 MeV. An important benefit when implementing spectrum tailoring is the neutron boost obtained from (n, 2n) reactions. The maximum intensity source strength anticipated using DT technology is ~2x10$^{12}$ n/s, to be conservative we assume a strength of ~10$^{11}$ n/s in the present paper.

### Concept of Plutonium Effective Mass to determine the fissile content in spent fuel

A DN-DDA instrument isn't capable of discerning what DN or PN came from which isotope, thus what is measured is a weighted average of all that fission referred to as the fissile content. In passive neutron

coincidence counting (PNCC) the concept of "$^{240}$Pueff"[19] was introduce in a similar context. We will use a similar term called "$^{239}Pu_{DN\text{-}eff}$" which stands for "$^{239}$Pu delayed neutron effective mass" defined in Equation 1.

$$^{239}Pu_{DN-eff} = C_1\,{}^{235}U + {}^{239}Pu + C_2\,{}^{241}Pu$$

**Equation 1**

$^{235}$U, $^{239}$Pu and $^{241}$Pu are masses calculated via CINDER.[12] The constants $C_1$ and $C_2$ weight the relative contribution of each isotope on a per gram basis. The way these factors are quantified is described later. They partition the signal but the effective mass also provides a convenient parameter against which to correlate the response.

**Monte Carlo Code Specifics and Post Tally Processing**

Physical processes were modeled in a faithful geometrical representation using MCNPX[15] (v27c).

*1. Delayed Neutron Count Rate*

Reactions in $^{3}$He were tallied using a F4 card (DN count rate (DNCR)/source neutron). The probability of a neutron being detected in a particular time interval per source neutron emitted was tallied from 1 to 300 seconds. We consider according to the delayed neutron time signature[7] that from 0 to 1 second the signal essentially comes from PN where it is made of DN in the later ones.

*2. Tally Multiplier in the fuel: Flux*

A tally multiplier, FM4, in the fuel provides neutron fluxes in the fuel and allows to determinate $C_1$ and C2 from Equation 1 using the following calculated number of total number of fission neutron (Equation 2a.) in a given time bin and as a result they are calculated in Equation 2b.

$$Total\ \#\ of\ \ fission\ neutrons_i = \iiint_{t\,V\,E} \Phi(\nu\sigma_f)_i\, dEdVdt \qquad \text{a.}$$

$$C_1 = \frac{A_{239}\beta_{235}\iiint_{t\,V\,E}\Phi(\nu\sigma_f)_{235}\,dEdVdt}{A_{235}\beta_{239}\iiint_{t\,V\,E}\Phi(\nu\sigma_f)_{239}\,dEdVdt} \quad and \quad C_2 = \frac{A_{239}\beta_{241}\iiint_{t\,V\,E}\Phi(\nu\sigma_f)_{241}\,dEdVdt}{A_{241}\beta_{239}\iiint_{t\,V\,E}\Phi(\nu\sigma_f)_{239}\,dEdVdt} \qquad \text{b.}$$

**Equation 2**

$\Phi$ (particles/cm$^2$) is the flux in the fuel. Since multiplication in the fuel and absorption by neutron absorbers both alter the interrogating flux, thus $\Phi$. V (cm$^3$) is the volume of the fuel over which the measurement takes place and E (MeV) is the neutron energy. $\sigma_f$ (barn) is the microscopic fission cross-section and $\beta$ the average number of DN emitted per fission over the whole energy range.[7] All terms are from MCNPX calculations[15] apart from $\beta$. The uncertainty in this tally is +/-0.11% rsd on the total flux in a given SFA. The early bin, built of PN, is processed in order to get $C_1$ and $C_2$ for DN by correcting the results by the DN fraction to determine the DN flux in later DN time bins.

*3. Tally Tagging in the detectors: Isotopic Contribution to the signal*

A tally, F4, provides the results as a detected fraction, efficiency included, which is the extent in which an isotope contributes to the detected signal. This fraction is normalized by the mass of the isotope, i, it weights. In this case, the "early bin", 0 to 1 s will also be used in order to get the DN isotopic contribution.

$$Isotopic\ Contributi\ on_i = SS \times \beta \times \frac{(Detected\ Fraction)_i}{m_i} \times (Atom\ Fraction)_i$$

**Equation 3**

The atom fraction per layer, pin, SFA and isotope is calculated in the code in *print table 40*. Masses are from CINDER.[12] The uncertainty on this tally is <0.85% on the overall number of neutrons tagged and to which a fraction of the flux is attributed. This uncertainty is larger since it includes the efficiency of the DN instrument.

**Counting statistics**

Uncertainties applied to the DNCR have been determined in 2 manners, calculated and measured, respectively representing the reality of experiments as in Equation 4 higher precision due to the many counting cycles, and the Monte Carlo uncertainties, where correlated results increase the error as in Equation 5 on the build-up of the DNCR over the 300 s data acquisition time (150 cycles of DN counting) in the simulations.

$$\sigma\left(\sum_{n=1}^{150} L_n\right)_{MEAS} = \sqrt{\sum_{n=1}^{150} \left(\sigma_{L_n}\right)^2}$$

**Equation 4**

$$\sigma\left(\sum_{n=1}^{150} L_n\right)_{CALC} = \sqrt{\sum_{n=0}^{149} \left((150 - n) \times \sigma_{K_{n+1}}\right)^2}$$

**Equation 5**

Where $L_n$ is the total number of counts in a cycle, n = 1 to 150 cycles and $K_n$ the tally results in a given bin which added-up provides $L_n$. The details are developed in the publication from Blanc et al.[8]

**Signal to background ratio**

The spontaneous fission (SF) activity of SFAs results in a high level neutron background that must be overcome. The main concern is related to the DN instrument since the PN yield is higher and benefit from the gating and thus a source strength chosen for DN would work in a DDA instrument a fortiori. The passive background comes from SF of mainly $^{244}$Cm and to a smaller extent (α, n) reactions which is a strong function of burnup. However (α, n) reactions in $^{17}$O and $^{18}$O can be assumed as a constant background intrinsic to the fuel assembly and therefore can be determined separately from experiments. The neutron source from spontaneous fission in $^{252}$Cf and $^{242}$Cm are negligible for SFAs with substantial CT; however there is a high build up of $^{244}$Cm which decays with a 18 years half-life through spontaneous fission. The optimum source strength explored seems to stand between 5x10$^{10}$ and 10$^{11}$ n/s to achieve a signal to background (S/B) ratio of ~30 % for a SFA burnt at 45 GWd/tU, 4% IE and 5 year CT since it is clearly visible and moreover relatively immune to non-statistical source of uncertainty such as positional error. In Figure 6 S/B ratios for SFAs with a S/B ratios > 40% at 5x10$^{10}$ n/s are displayed.

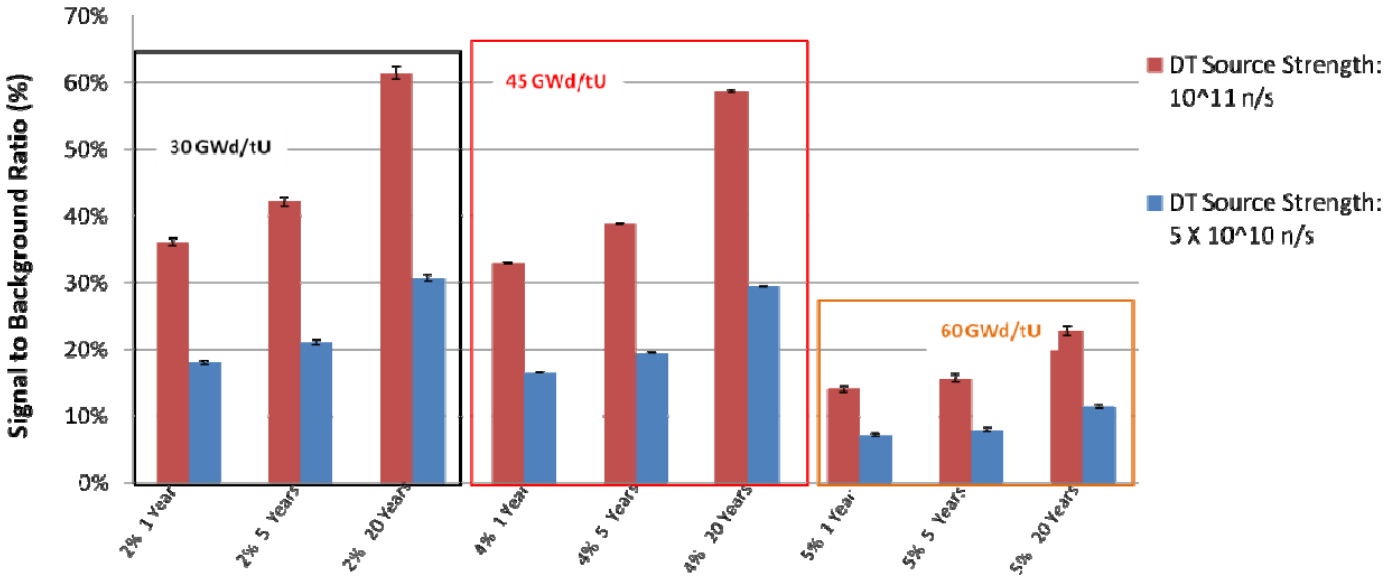


Figure 6: S/B ratio for ~10$^{11}$ & ~5x10$^{10}$ n/s source strengths. SFAs from the spent fuel library with S/B ratio <40% (at 5x10$^{10}$ n/s). Uncertainties are measured from Equation 4.

Although a DT source strength of ~5x10$^{10}$ n/s would probably be sufficient for the reference assembly, ~10$^{11}$ n/s will be assumed in the following steps. At high BU, 60 GWd/tU, corresponding to a lower amount of fissile materials and higher passive signal, it is harder to discriminate the SF background and a ~10$^{11}$ n/s source strength may be more appropriate.

**Sensitivity of the delayed neutron instrument to diversion of fuel pins**

Nine diversion scenarios have been created.[17] The 3 original assemblies had 4% IE and 5 year CT, with BU of 15, 30 and 45 GWd/tU. In each scenarios, fuel pins were replaced with pins containing depleted uranium (DU) consisting of 0.2 weight percent $^{235}$U. They were removed from 1 of 3 (inner, middle, and outer) regions in the 17x17 array of fuel pins. 8, 24 and 40 pins removal have been simulated from the different regions. In Table 1 The negative percentages represent the drop in the count to the "normal" case where no pins have been replaced. In red are cases where the DNCR drop gives a response that stands in the calculated (from Equation 5) standard deviation multiplied by 3 of the "normal" case and thus we consider the instrument blind to these 3 scenarios. This method of assessment allows us to achieve a level of precision insuring a degree of confidence of ~99%.

Table 1: Drop in the counts from base case (no pins replaced) to each of the 9 diversion cases[17], replacing 8, 24 and 40 pins in 3 regions, middle, inner and outer. RSD multiplied by 3 measured and calculated. 3 fuel assemblies: 15, 30 and 45 GWd/tU BU, IE=4% & CT=5 years.

| | | | Percent Difference from Intact | | |
|---|---|---|---|---|---|
| **Diversion:# of pins** | **Region** | **%Mass Diverted** | **15GWd/tU** | **30GWd/tU** | **45GWd/tU** |
| | | | **Measured** | **Measured** | **Measured** |
| **Normal** | **–** | **–** | **RSDX3=0.14%** | **RSDX3=0.15%** | **RSDX3=0.16%** |
| | | | **Calculated** | **Calculated** | **Calculated** |
| **Normal** | **–** | **–** | **RSDX3=1.70%** | **RSDX3=1.85%** | **RSDX3=1.90%** |
| 8 pins | Middle | 3.0% | -5.03% | -2.81% | **-0.43%** |
| 24 pins | Middle | 9.1% | -21.01% | -12.69% | -7.08% |
| 40 pins | Middle | 15.2% | -40.19% | -26.81% | -17.68% |
| 8 pins | Inner | 3.0% | -3.95% | -2.85% | **-0.24%** |
| 24 pins | Inner | 9.1% | -14.94% | -8.79% | -4.84% |
| 40 pins | Inner | 15.2% | -25.27% | -16.28% | -10.05% |
| 8 pins | Outer | 3.0% | -3.92% | -2.90% | **-1.67%** |
| 24 pins | Outer | 9.1% | -11.79% | -7.91% | -4.94% |
| 40 pins | Outer | 15.2% | -20.38% | -15.00% | -9.26% |

The 3 most critical scenarios are when 8 pins in the 3 regions, middle, inner and outer have been replaced. As BU increases the ability to detect diversion decreases. For other scenarios where the FA is burnt at 15 and 30 GWd/tU, diversion is well outside the range of systematic uncertainty and in the absence of other, yet to be identified, we expect that the DN instrument will be able to detect these diversions. For 45 GWd/tU burnt SFAs, removing 40 pins from any region is easily detectable as well as 24 from the inner.

**Spatial responses of the DN-DDA signals**

Six simulations consist in replacing 11 fuel pins at 6 locations of the SFA with DU (0.2 weight percent $^{235}$U), black pins in Figure 7. The "base case" is when no pins have been replaced. 9 locations are north-west (NW), north (N), north-east (NE), west (W), central (C), east, south-west (SW) and south-east (SE). Half has been performed since the DN instrument is symmetric in the Y direction.

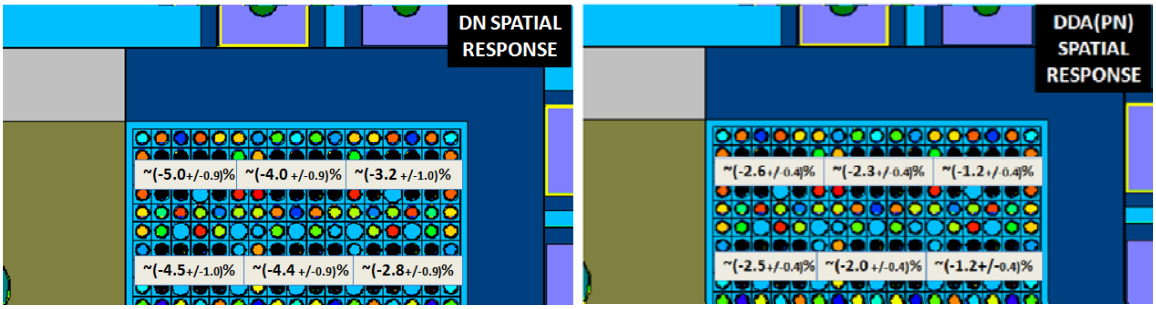


Figure 7: From left to right, drop in counts from base to spatially replaced case for DN&PN detection. Colored pins=fuel pins. Blue=water guide pins. Black=replaced by DU pins. 6 locations - 11 pins replaced. Uncertainties calculated (Equation 5).SFA: 45 GWd/tU, 4% IE & 5 yr CT. For DDA(PN) the time gate is from 20 to 200 μs.

Figure 7 represents the percentage of drops in the delayed and prompt neutron count rates for a fuel assembly burnt at 45 GWd/tU, cooled during 5 years and with an initial enrichment of 4% from the base case where no pins have been replaced to each of the 6 cases. A relatively smooth response is obtained when counting DN.

The DDA instrument gives the results in the 20 to 200 μs time gate. Detection of diversion appears to be achievable that way, however to measure the fissile content, a detailed study is part of the ongoing research. In early bins such as 20 to 200 μs, source neutrons may be a background to the signal of interest. However source neutrons have a die-away time of ~70 μs therefore at later time they remain as thermal neutrons and are eliminated by the Cd, at earlier time like 20 μs, source neutrons detected are the epi-cadmium flux and the die-away time in Cd is only 2-3 μs therefore the initial source neutron population will have dropped of ~50 die-away times and should be negligible especially compared to the fission activity undergoing a very high multiplication. However the distribution of the source neutrons over time together with a study of a wider range of time windows will be performed in order to determine also the fissile content properly and furthermore the impact of the increase of the poison population with CT and BU on the signal of interest in later bins since neutrons will have lived longer in the fuel and cold neutrons are more sensitive to poisons. In Figure 7 the goal is to assess the spatial response of the fuel where PN seem to have a similar behavior than DN and to be rather smooth.

The DN instrument doesn't need Cd around its detectors the counting gate being opened at 1 s which is ~$14 \times 10^3$ time higher than the die-away time of SN and makes their impact negligible. In Figure 8 the contribution to the DNCR in each detector is represented for DN and PN detections in order to determine more accurately how the fuel responds. Especially in the context of PN, it will allow us to observe and explore the penetrability of the fuel.

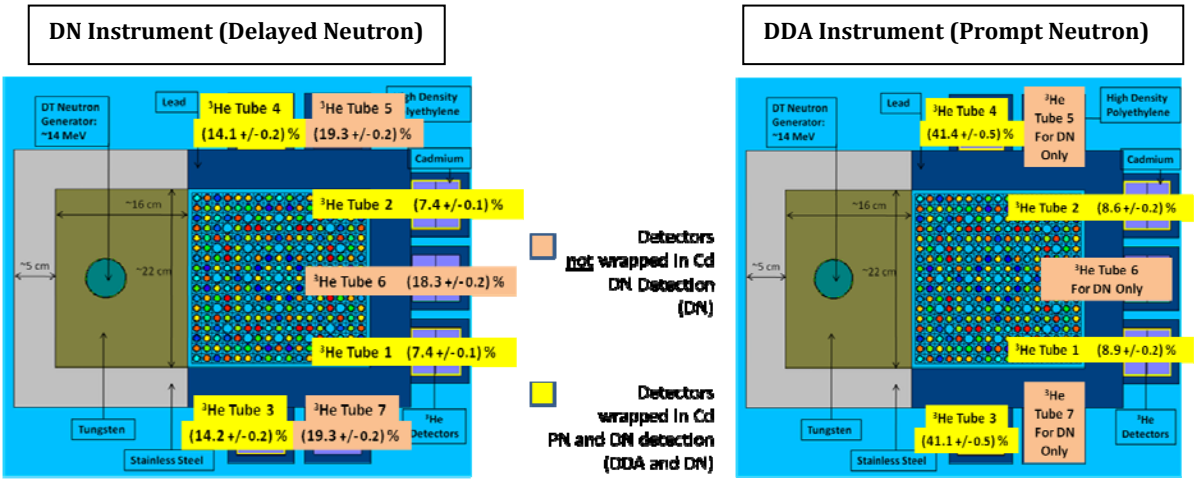


Figure 8: 7 $^3$He proportional counters are numbered and their contribution to the total DNCR is specified. From left to right the DN and DDA (20 to 200 μs gate).$^3$He tubes wrapped in Cd (tubes 1 to 4) are used for PN detections only. Uncertainties calculated and propagated (Equation 5).

When counting DN, the 4 detectors, Tubes 5 to 7, not wrapped in Cd, are more efficient for DN counting than tubes 1 to 4 are. Symmetry in the Y direction of the DDA and DN instruments provides statistically equal contributions in the couple of tubes (5, 7), (1, 2) and (3, 4). When it comes to DDA (PN), signals from tubes 5 to 7 is ignored since they wouldn't discriminate low energy neutrons and therefore wouldn't give any useful information regarding prompt neutrons. The contributions behaviors (Figure 8) together with the spatial variability of the fuel response (Figure 7) are the key parameters to optimize an integrated instrument. When looking at the contribution of each detector in the back in later bins, 200 to 1000 µs, in tubes 4 and 3 it decreases to ~30% and increases in 1 and 2 to ~20% from Figure 8 (20 to 200 µs). Thus going later in time is favorable to the back of the system for prompt neutrons. A way to improve the spatial response for DDA staying in earlier bin would be to increase the efficiency in the back by wrapping up the 3 other $^{3}$He detectors in Cd. However it would decrease the efficiency of the DN sensitivity to diversion in the back, nevertheless the difference from ~7.3% to 18.3% of contribution from the middle detector to the 2 others is not only due to efficiency from the absence of Cd but also from higher multiplication at this location, thus the overall could be balanced and also thanks to the fact that the front response for DN may also be decreased by the presence of Cd around the 2 other side detectors. Further research to explore and correlate all these parameters is undergoing.

**Delayed Neutron Intensity as a Function of $^{239}Pu_{DNeffective}$**

The DN count rate decreases as the burnup increases since neutron absorbers population increases and the fissile content decreases. The variation in the delayed neutron count rate as a function of burnup confirms the dominance of $^{235}$U as compared to the fissile isotopes of Pu. The change in the delayed neutron count rate is more rapid at low burnup since $^{235}$U is the dominant fissile isotope, and as such, it is being depleted at a faster rate. Later in time (when the burnup is higher) $^{239}$Pu, $^{241}$Pu and $^{235}$U are being consumed to maintain the power output of the reactor. The percentage change in the delayed neutron count rate with cooling time at 15 GWd/tU is significantly smaller than at 60 GWd/tU. This behavior is due to two primary factors, the percentage of the count rate from $^{241}$Pu is the greatest at high BU since $^{241}$Pu has a 14 years half-life, the loss of it is noticed more at elevated burnup and where there is more $^{155}$Gd and $^{241}$Am so the impact of these two neutron absorbers is greater. In minimizing fission of fertile isotopes, mainly $^{238}$U, the ideal outcome would be to observe that the DN count rate scales primarily with the weighted masses of the fissile isotopes $^{235}$U, $^{239}$Pu, and $^{241}$Pu. In Figure 9 the delayed neutron count rate is graphed as a function of the "Fissile Content $^{239}Pu_{DN\text{-}effective}$" for each of the 64 assemblies[17] in water. In order to determine it Equation 1 and Equation 2 are used.

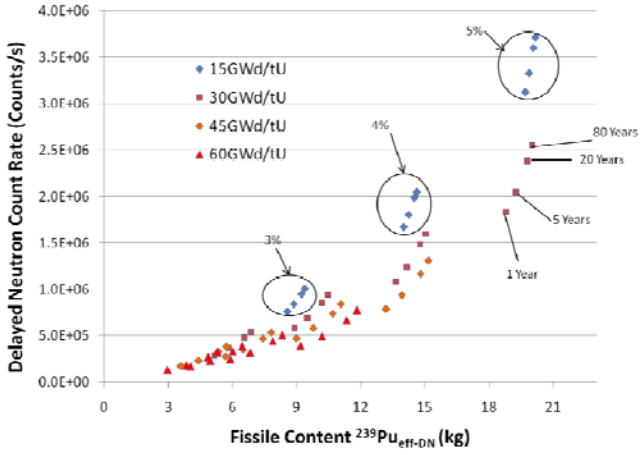


Figure 9: DN count rate as a function of the fissile content - mass of $^{239}Pu_{eff\text{-}DN}$ for the 64 fuel assemblies of the spent fuel library[17] representing 4 BU, 15, 30, 45 and 60 GWd/tU, 4 CT, 1, 5, 20 and 80 years and 4 IE, 2, 3, 4 and 5%.

Each data point in Figure 9 represents an assembly with a wide range of actinides and fission products. It can be seen that "$^{239}Pu_{DN\text{-}effective}$" scales in a uniform manner with the DNCR. It appears that all 64 data points do not fit on a smooth curve; instead, there is structure that is dependent on cooling time, burnup and initial enrichment. We also expect that some form of correction for the buildup of neutron absorbers is needed in order to get a smoother relationship between count rates and the fissile content expressed in term of "$^{239}Pu_{DN\text{-}effective}$". That should be subject to further optimization of the simulation results treatment. The isotopic contributions of the 3 fissile, $^{235}U$ $^{239}Pu$ and $^{241}Pu$ and of main fertile $^{238}U$ are shown in Figure 10 through Equation 3.

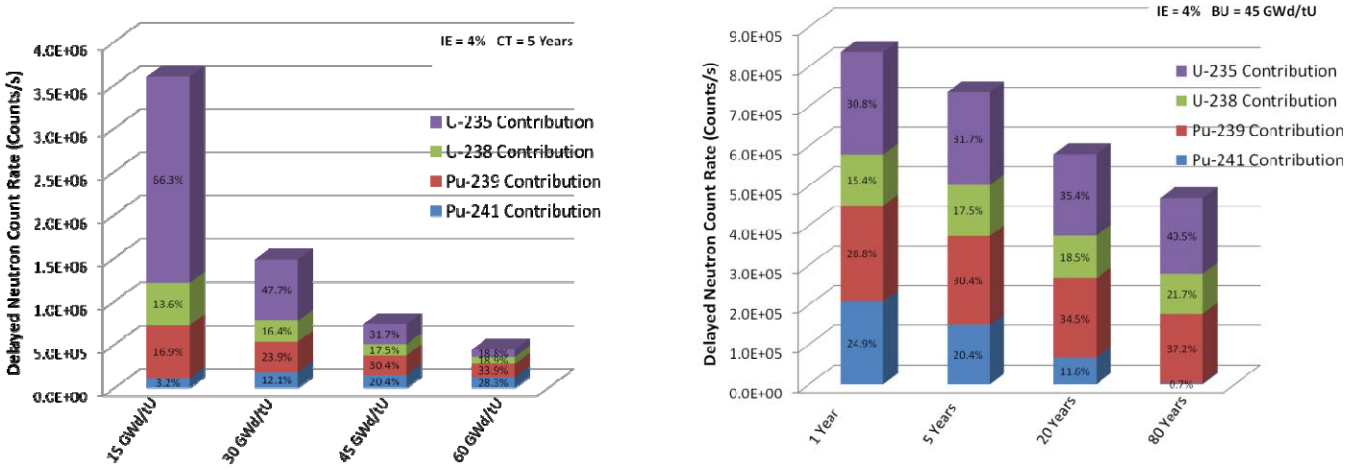


Figure 10: From left to right, isotopic contributions of the 3 main fissile, $^{235}U$, $^{239}Pu$ and $^{241}Pu$ and main fertile $^{238}U$ to the total DNCR respectively as a function of BU and CT for an IE fixed to 4% and for a CT fixed to 4% and a BU fixed to 45 GWd/tU. In both figures, contributions are represented in purple, green, red and blue for respectively $^{235}U$, $^{239}Pu$, $^{241}Pu$ and $^{238}U$.

The mass of $^{238}U$ is nearly constant in all assemblies. The change in its count rate is due primarily to reduced multiplication. Since the delayed neutron production from $^{238}U$ falls roughly in half as the multiplication goes from ~4 to ~1.5, this indicates that the fission of $^{238}U$ by neutron directly originating in the neutron generator is less than half of the fissions in $^{238}U$. Figure 10 (right) indicates that for a given assembly, the relative contributions of $^{235}U$, $^{239}Pu$, and $^{238}U$ stay constant or of the same order of magnitude, indicating that the quantities that change with time (neutron absorbers masses and $^{241}Pu$ mass) do not change the relative contribution of $^{235}U$, $^{239}Pu$, and $^{238}U$ as a function of cooling time. Figure 10 indicates that as the assembly burns the DN contribution from $^{235}U$ goes from being dominant (greater than 65%) to a nearly equivalent point or comparable to the other three main isotope contributions.

**Summary**

Further work has to be performed exploring the DN and DDA instrument separately, in order to determine their capability in other media such as air or borated water, quantifying with accuracy the active backgrounds contributing to the delayed neutron signal and biasing the fissile content determination and neutron absorbers influence on the absolute signal contributions should also be explored with precision for both techniques. Moreover, work on integrating both techniques in common simulations is the next step of this research in order to prepare for experiments. However, one main challenge remains, and lies in the fact that the irradiation time required for DDA is much shorter than for DN. Thus, in an application that made use of both DN and PN, the DN

will determine the required (D, T) source strength to override the $^{244}Cm$ background, and the measurement run time. But regarding the first results developed in this paper, these techniques (PN and DN) seem to be compatible on many levels for integration. Thus, it seems achievable to technically combine both signatures for the goal of quantifying both the uranium and plutonium fissile content in spent nuclear fuel assemblies.

**Acknowledgements**

The authors would like to acknowledge support from the Next Generation Safeguards Initiative (NGSI) of the U.S. Department of Energy. Pauline Blanc would like to thank Dr. Howard O. Menlove with whom I have had the immense honor to work and from whom I have learnt a lot thanks to his passion to teach and share his immense knowledge. She is also thankful to the support of Vladimir Mozin, Jianwei Hu, Martyn Swinhoe and Taehoon Lee with whom we have worked as a team throughout the many projects.

## REFERENCES

1. S.J. Tobin, S.F. Demuth, M.L. Fensin, J.S. Hendricks, H.O. Menlove, M.T. Swinhoe, "*Determination of Plutonium Content in Spent Fuel with NDA – Why an Integrated Approach?*." Annual Meeting of the Institute of Nuclear Material Management, Nashville, TN, July 2008 (LA-UR-08-03763).
2. Menlove, H. O., Baca, J., Krick, M. S., Kroncke, K. E., &Langner, D. G. (1993) "*Plutonium Scrap Multiplicity Counter Operation Manual*".
3. Conlin, J. L. & Tobin, S. J. (2010) "*Determining Fissile Content in PWR Assemblies Using a Passive Neutron Albedo Reactivity Technique*".
4. Pelowitz, D. B., James, M. R., McKinney, G. W., Durkee, J. W., Fensin, M. L., Hendricks, J. S., Mashnik, S. G., & Waters, L. S. (2009) MCNPX 2.7.B Extensions.
5. (1991) "*Passive Nondestructive Assay of Nuclear Materials*".
6. Fensin, M. L., Tobin, S. J., Sandoval, N. P., Thompson, S. J., &Swinhoe, M. T. (2009) "*A Monte Carlo Linked Depletion Spent Fuel Library for Assessing Varied Nondestructive Assay Techniques for Nuclear Safeguards*."
7. P. M. Rinard, "*Application Guide to Shufflers*", Los Alamos National Laboratory Report, LA-13819-MS, (2001).
8. P. Blanc, S. J. Tobin, T. Lee, J. Hu, J. Hendricks, S. Croft (2010) "*Delayed Neutron Detection with an Integrated Differential Die-Away and a Delayed Neutron Instrument*." Los Alamos National Laboratory, LA-UR 10-04125, 51st INMM, July 11-15, Baltimore, MD.
9. C.J. Werner "*Simulation of Delayed Neutrons Using MCNP*", Progress In Nuclear Energy, Vol. 41, PJI: S0149-1970(02)00019-7, 2002 Elsevier Science.
10. D.D. Cobb, J.R. Philips, M.P. Baker, G.E. Bosler, G.W. Eccleston, J.K. Halbig, S.L. Klein, S.F. Klosterbuer, H.O. Menlove, C.A. Ostenak, C.C. Thomas, Jr., "*Nondestructive Verification and Assay Systems for Spent Fuels*", Los Alamos National Laboratory, LA-9041 Vol. 2. April 1982.
11. ENDF VII from www.lanl.t2.gov
12. M.L. Fensin, J.S. Hendricks, S. Anghaie, "*The Enhancements and Testing for the MCNPX 2.6.0 Depletion Capability*", Nucl. Technol. 170, 1, p.68-79 (2010).
13. J. M. Campbell (XCI), G. D. Spriggs (XNH), "*8 groups delayed neutron spectral data for Hansen-Roach energy group structure*", Los Alamos National Laboratory, LA-UR-99-4000, (1999)
14. J. M. Campbell (XCI), G. D. Spriggs (XNH), "*Delayed neutron spectral data for Hansen-Roach energy group structure*", Los Alamos National Laboratory, LA-UR-99-2988, (1999)
15. J. F. Pelowitz (Editor), "*MCNPX™ USER'S MANUAL Version 2.5.0*," Los Alamos National Laboratory report LA-CP-05-0369 (2005).
16. T. Lee, H. O. Menlove, M. T. Swinhoe, S. J. Tobin, "*Differential Die-Away technique for determination of the fissile contents in spent fuel assembly*." Los Alamos National Laboratory, 51st INMM, July 11-15, Baltimore, MD.
17. M.L. Fensin, S.J. Tobin, N.P. Sandoval, M.T. Swinhoe, S.J. Thompson, "*A Monte Carlo linked Depletion Spent Fuel Library for Assessing Varied Nondestructive Assay Techniques for Nuclear Safeguards*." Advances in Nuclear Fuel Management IV (ANFM), Hilton Head Island, South Carolina, USA, April 12-15, 2009.
18. H. O. Menlove, R. H. Augustson, D. B. Smith, "*A multi-spectra neutron irradiation technique for the nondestructive assay of fissionable materials.*" Nuclear Technology Vol. 10 (1971).
19. S. Croft, P. Blanc, N. Menaa, "*Precision of the Accidentals rate in neutron coincidence counting-10475*", Canberra industries inc., WM'10, March 07, 2010, in Phoenix, AZ.